*Highlights of Spanish Astrophysics XII, Proceedings of the XVI Scientific Meeting of the Spanish Astronomical Society held on July 15 - 19, 2024, in Granada, Spain. M. Manteiga, F. González Galindo, A. Labiano Ortega, M. Martínez González, N. Rea, M. Romero Gómez, A. Ulla Miguel, G. Yepes, C. Rodríguez López, A. Gómez García and C. Dafonte (eds.), 2025*

# Satellite quenching in a suite of cosmological zoom-in simulations of a Milky Way-mass halo: a new project within the *AGORA* Collaboration

**Rodríguez-Cardoso, R.[1,2], Roca-Fàbrega, S.[3], Gallego, J.[1] and the AGORA Collaboration**

[1] Departamento de Física de la Tierra y Astrofísica, Universidad Complutense de Madrid, Facultad de Ciencias Físicas, Plaza Ciencias, 1, 28040 Madrid, Spain
[2] GMV, Space and Avionics Equipment, Isaac Newton, 11 Tres Cantos, E-28760 Madrid, Spain
[3] Lund Observatory, Department of Astronomy and Theoretical Physics, Lund University, Box 43, SE-221 00 Lund, Sweden

## Abstract

In this work, we analyze satellite quenching in a subset of the high-resolution cosmological hydrodynamic zoom-in simulations of a Milky Way(MW)-mass halo from the AGORA CosmoRun. These simulations model the same MW-like halo using some of the most widely used codes, each applying its own stellar feedback physics. By studying the convergence and divergence of the results, we identify which outcomes are code-independent and which parameters are most sensitive to variations in the stellar feedback recipes and the code architecture. In general, we have observed convergence across codes regarding the overall trends in quenching timescales and quenched fractions, despite the use of different approaches for supernova feedback: the less massive the satellite, the faster its quenching occurs. We also found that ram pressure stripping and strangulation are the most dominant mechanisms driving satellite quenching in MW-mass halos, regardless of the code or supernova feedback recipe employed (although their efficiency is highly dependent on the feedback model). On the other hand, beyond these general trends, the specific quenching timescales and the fraction of quenched satellites with stellar masses above $10^7\, M_\odot$ are highly sensitive to the different feedback implementations considered in CosmoRun.

## 1 Introduction

Cosmological hydrodynamic simulations are the best tool available for interpreting astrophysical observations. While many groups are developing codes in order to focus on whether galactic astrophysics can realistically reproduce galaxies, a key question remains: do these shared physics yield consistent results across different simulation codes? AGORA was founded to analyze this question and foster collaboration among code developers to make simulations comparable and consistent.

In this work, we use a subset of the AGORA CosmoRun high-resolution cosmological hydrodynamical simulations presented in [4, 5], where the same Milky Way-mass halo ($M_{halo} \sim 10^{12}\, M_\odot$ at $z = 0$) is simulated starting from identical initial conditions and keeping the baryonic physics as consistent as possible. The only variation lies in the supernovae feedback recipe, with each code group using the one most commonly employed in their respective codes.

Satellite galaxies are expected to undergo a variety of physical processes during their infall to their host haloes. Theoretical models predict that these effects will be particularly significant when the host halo reaches a critical mass of a few times $10^{11} M_\odot$, at which point virial shocks are expected to form within the host halo. Due to the formation of these virial shocks, a warm-hot gas corona develops, preventing the accretion of the cold gas necessary for star formation. In addition to this cut-off of cold inflows in the satellites, as they move through the hot circumgalactic medium (CGM), they may lose gas due to ram pressure stripping, tidal stripping and/or harassment. These processes are expected to quench satellites, explaining the high fractions of quenched galaxies in Local Group (LG) satellite population. However, the interplay between these mechanisms in MW-mass halos remains under debate. As the halos in CosmoRun reach the mass predicted by theory for virial shock formation at $z \sim 1$, studying satellite quenching at low redshift provides a suitable scenario to test how they are affected by the host's CGM. We analyze satellite quenching in this suite of simulations in order to determine whether quenched fractions, quenching timescales and the dominant quenching mechanisms are consistent across codes or if they show sensitivity to the specific supernovae feedback physics employed.

## 2 Results

### 2.1 Satellite quenched fraction across host halo evolution

In Figure 1, by comparing the different quenched fraction in both satellite (top) and field (bottom) galaxies for all the codes, we identify how the evolution of the host CGM influences satellite properties in contrast to dwarf galaxies population not affected by the central galaxy.

We identify some convergences across all models: low-mass subhalos ($M_{peak\, halo} < 10^{10}\, M_\odot$) undergo quenching earlier than high-mass subhalos ($M_{peak\, halo} < 10^{10}\, M_\odot$). The $f_{q,\, sat}$ for them is higher than that for high-mass subhalos throughout all the evolution, suggesting that the quenching mechanism is both more effective and rapid for low-mass subhalos. Indeed, $f_{q,\, sat}$ for low-mass satellites is consistently higher than $f_{q,\, field}$ for low-mass field galaxies since when the host halo mass surpasses $5 \cdot 10^{11}\, M_\odot$ (orange shaded region). Attending to the more massive satellite galaxies, they only quench when the host halo exceeds $10^{12}\, M_\odot$ (red shaded region). Meanwhile, the field galaxies with the same mass remain star-forming.

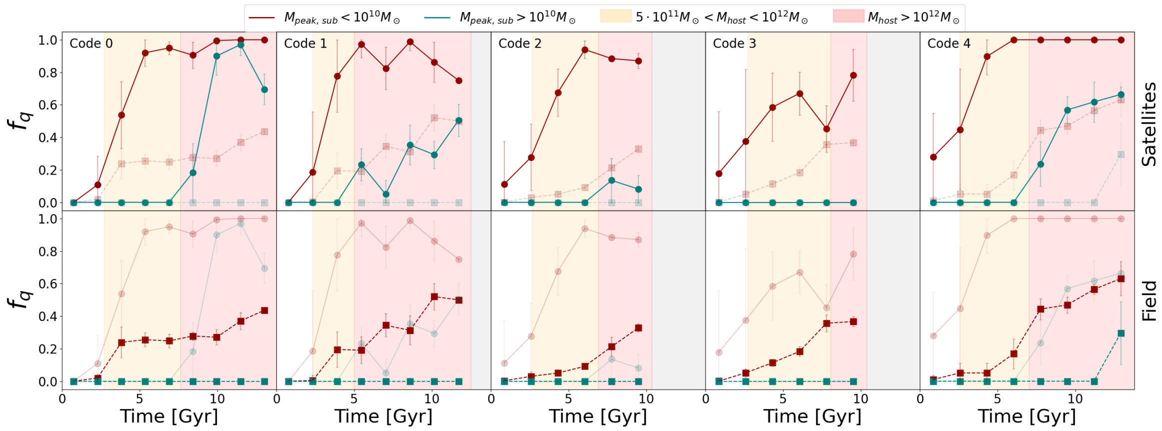


Figure 1: The evolution of the fraction of quenched satellite galaxies (**top**) across cosmic time against the one for field galaxies (**bottom**) for each model. The orange and red shaded regions represent the epochs when the host halo is more massive than $5 \cdot 10^{11}\, M_\odot$ and $10^{12}\, M_\odot$, respectively. The time domain where snapshots are still not available for each specific code are indicated as a grey shaded region. Quenched fractions for satellite galaxies and field galaxies above and below $M_{peak} = 10^{10} M_\odot$ are shown in different colors.

On the other hand, we identify some discrepancies between models. $f_{q,\,sat}$ differ among models, particularly for high-mass subhalos. While CODE 0 and CODE 4 achieve $f_{q,\,sat}$ above 80% and 60%, respectively, for high-mass subhalos at $z \sim 0.3$, CODE 2 barely exceeds 15% and CODE 3 is not able to quench any subhalo above $M_{peak} = 10^{10}\, M_\odot$.

### 2.2 When do satellites quench?

By analyzing the quenching delay time since infall to the host halo vs the satellite stellar mass in Figure 2 we show that all the models follow the same trend identified in observations: the less massive the satellite galaxy is, the faster its quenching. Satellites with stellar masses above $10^7\, M_\odot$ are resistant to rapid environmental quenching for all the models, whereas satellites below $10^7\, M_\odot$ are compatible with fast and efficient quenching showing quenching delay times below $\sim 2\,$Gyr.

Some discrepancies between models can be highlighted. The CODE 0 model is the only one that quenches satellites with masses above $10^8\, M_\odot$, while for the rest of the models all galaxies with masses above this limit remain star-forming, similar to the findings in [1]. CODE 3 and CODE 2 have a higher abundance of star-forming galaxies, pointing to higher quenching delay times than the other models. In addition, CODE 3 also has a higher number of satellites that were disrupted prior to quenching, indicating differences in satellite-host interactions relative to the other models.

Many of the lowest-mass satellites, below $\sim 10^6\, M_\odot$, undergo quenching before infall. Environmental mechanisms beyond $R_{vir}^{host}$ as ram pressure stripping or harassment can effectively quench low-mas satellites. However, there are many potential mechanisms, not related

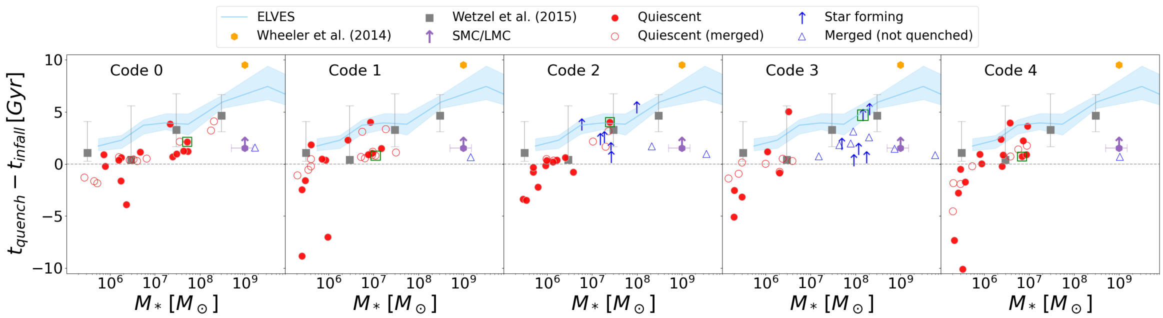


Figure 2: Satellites quenching delay time as function of their stellar mass. Quenched satellites are represented by red filled circles, while star-forming satellites are indicated by blue arrows, marking a lower limit on their quenching delay times. Satellites that merged when $M_{host} > 5 \cdot 10^{11}\, M_\odot$ are also shown: red open circles denote those quenched before merging, and blue open triangles denote those that were not (they still have either ongoing star formation or star-forming gas reservoirs at the time of merger). Observational estimates from [7], and [8] are shown in grey squares and orange hexagons, respectively. An estimate of the quenching timescale for the SMC/LMC system is shown in purple, using the infall time predicted by [3]. The quenching time for the ELVES survey [2] is also shown in blue. The open green square enclosing a single data point in each panel indicates the same satellite across the different models and we compare its evolution in Figure 3.

to the influence of the host, for the early quenching of these low-mass galaxies as: cosmic reionization, UV background heating or pre-processing in low-mass groups.

## 2.3 How do satellites quench?

Different supernova feedback physics result in different gas mass and density across the CosmoRun models. This leads to different restoring pressures for each satellite in each code, which determines their ability to retain gas against stripping mechanisms during infall. While the ram pressure and tidal forces experienced by the gas of each satellite in each code are similar, the differing restoring pressures determine the quenching efficiency for each model. Figure 4 illustrates an example of how the gas content evolves during infall for the same satellite identified across all codes. Those models with higher gas mass and density retain their gas reservoirs, while others lose them quickly due to stripping processes.

In this work, we developed a methodology to quantify the contribution of the different quenching mechanisms considered (details in [6]). In Figure 4, we present Venn diagrams for each model, showing the fraction of satellites affected by each gas stripping mechanism considered. Strangulation is excluded for clarity, since it impacts all satellites.

The most common gas stripping mechanism across all models is ram pressure stripping, either acting alone or in combination with tidal stripping, and less frequently, with harassment. The exception to these results is CODE 3, the restoring pressure and gas mass of satellites with stellar masses above $10^7 M_\odot$ are higher than in the other codes, making ram

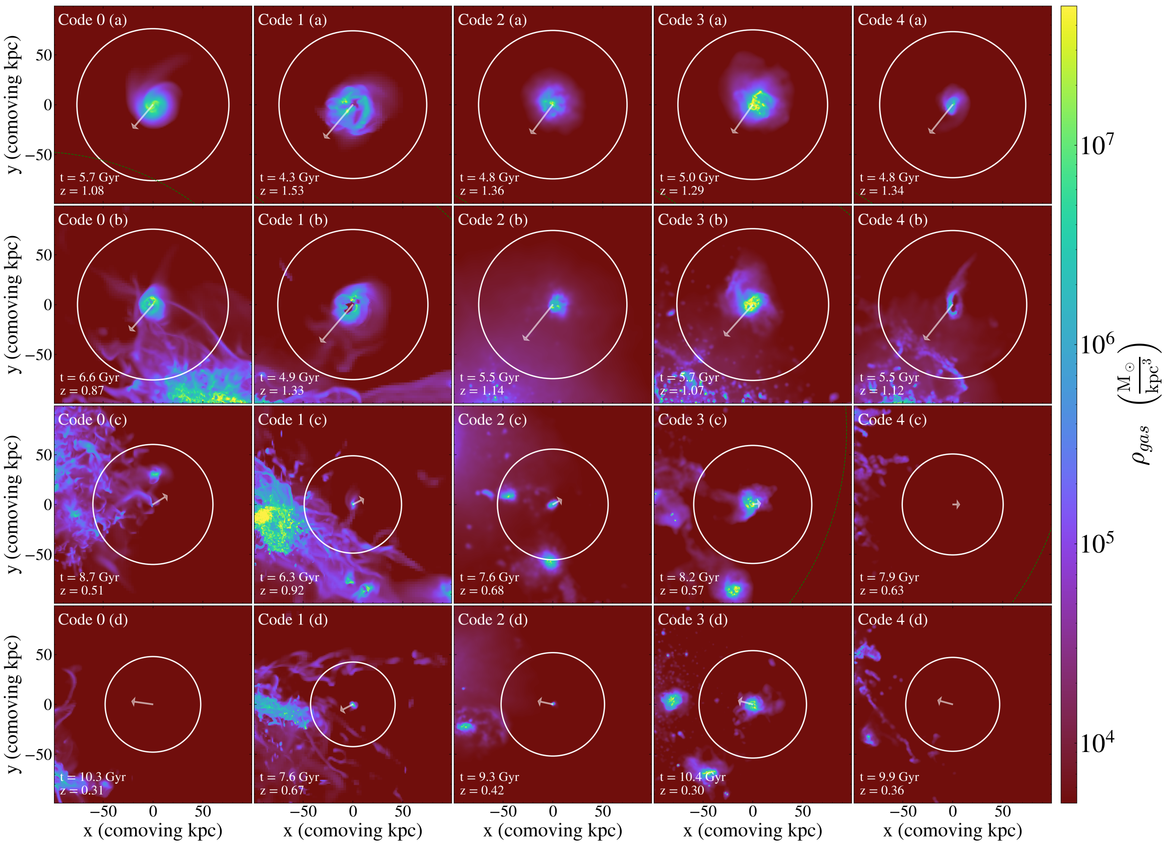


Figure 3: Gas density of the same subhalo across the different models during their infall to the host halo. Each column represent a different model, while each row indicates the same infall stage: **(a)** first snapshot at a distance to the host lower than $2R_{vir,host}$, **(b)** at $t_{infall}$, **(c)** during the first apocentre, and **(d)** during the second infall, slightly before the second pericentre. White solid circle show the subhalo virial radius, while the white arrow provides information about the subhalo's velocity, showing the predicted position of the center of the subhalo in 100 Myr assuming the same velocity as in the current snapshot.

pressure less efficient. Hence, in CODE 3, ram pressure and tidal forces are nearly equally relevant. Consistent with this, when comparing the percentage of satellites unaffected by any stripping mechanism, CODE 3 shows the highest proportion at 21%, as ram pressure stripping is inefficient for all satellites with masses greater than $10^7 M_\odot$. This is followed by CODE 2 with 15%, which also exhibits higher restoring pressures than the other models.

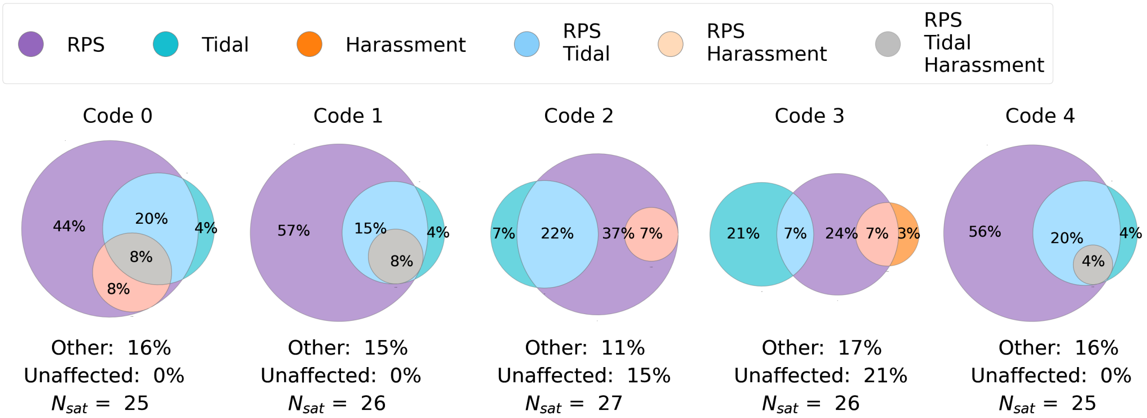


Figure 4: Venn diagram for each CosmoRun model showing the fraction of satellites affected by each of the mechanisms considered responsible for the stripping of the satellites' gas. All satellites shown in Figure 2 are included. Please note that we found that strangulation affects all satellites by cutting off the replenishment of cold gas reservoirs; however, since it impacts 100% of the satellites, we do not include it to enhance clarity. Below each diagram, we present the fraction of satellites quenched by other mechanisms not considered in our analysis, along with the fraction of satellites that are unaffected by any mechanism and still star-forming, and the total number of satellites analyzed.

## Acknowledgments

We thank all of our colleagues participating in the AGORA Project for their collaborative spirit, which has allowed the AGORA Collaboration to remain strong as a platform to foster and launch multiple science-oriented comparison efforts. This research used resources of the National Energy Research Scientific Computing Center, a DOE Office of Science User Facility supported by the Office of Science of the U.S. Department of Energy under contract No. DE-AC02-05CH11231. R.R.C. acknowledges financial support by the Spanish Ministry of Science and Innovation through the research grants PID2021-123417OB-I00 and IND2022/TIC-23643.

## References

[1] Akins, H.B., Christensen, C. R., Brooks, A. M., et al. 2021, ApJ, 909, 139

[2] Greene, J. E., Danieli, S., Carlsten, S. et al 2023, ApJ, 949, 94

[3] Kallivayalil, N., van der Marel, R. P., Besla, G., et al. 2013, ApJ, 764, 161

[4] Roca-Fàbrega, S., Kim, J-h. Primack, J.R., et al 2021, ApJ, 917, 64

[5] Roca-Fàbrega, S., Kim, J-h. Primack, J.R., et al. 2024, ApJ, 968, 125

[6] Rodriguez-Cardoso et al. in prep

[7] Wetzel, A. R., Tollerud, E. J., and Weisz, D. R. 2015, ApJ, 808, L27

[8] Wheeler, C., Phillips, J. I., Cooper, M. C., et al 2014, MNRAS, 442, 1396-1404